Cancer Research

Expression of Adipocyte/Macrophage Fatty Acid–Binding Protein in Tumor-Associated Macrophages Promotes Breast Cancer Progression

Jiaqing Hao[1], Fei Yan[2], Yuwen Zhang[1], Ashley Triplett[1,3], Ying Zhang[4], Debra A. Schultz[5], Yanwen Sun[1], Jun Zeng[1,6], Kevin A.T. Silverstein[4], Qi Zheng[7], David A. Bernlohr[8], Margot P. Cleary[2], Nejat K. Egilmez[1], Edward Sauter[9], Shujun Liu[2], Jill Suttles[1], and Bing Li[1]

Abstract

Tumor-associated macrophages (TAM) play a critical role in cancer development and progression. However, the heterogeneity of TAM presents a major challenge to identify clinically relevant markers for protumor TAM. Here, we report that expression of adipocyte/macrophage fatty acid–binding protein (A-FABP) in TAM promotes breast cancer progression. Although upregulation of A-FABP was inversely associated with breast cancer survival, deficiency of A-FABP significantly reduced mammary tumor growth and metastasis. Furthermore, the protumor effect of A-FABP was mediated by TAM, in particular, in a subset of TAM with a $CD11b^{+}F4/80^{+}MHCII^{-}Ly6C^{-}$ phenotype. A-FABP expression in TAM facilitated protumor IL6/STAT3 signaling through regulation of the NFκB/*miR-29b* pathway. Collectively, our results suggest A-FABP as a new functional marker for protumor TAM.

Significance: These findings identify A-FABP as a functional marker for protumor macrophages, thus offering a new target for tumor immunotherapy. *Cancer Res; 78(9); 2343–55. ©2018 AACR.*

Introduction

Breast cancer is the most common cancer in women worldwide and its incidence has increased dramatically from 641,000 cases in 1980 to more than 1.6 million in 2010 (1). Only in the United States, there are an estimated 249,260 new breast cancer cases in 2016 (2). Despite improvements in breast cancer screening and therapy, it still kills nearly half-a-million women annually, about 90% of whom die from distant metastases (3). Therefore, there is great interest in the identification of new cellular and molecular mechanisms that mediate breast cancer growth and metastasis.

It is well-documented that tumor stromal cells actively participate in tumor progression (4, 5). Tumor-associated macrophages (TAM) are the most abundant myeloid cells infiltrating the tumor microenvironment (6). Clinical and experimental evidence has shown that a high density of TAM is associated with both poor prognosis and decreased survival in breast cancer patients. Conversely, deletion of macrophages in mice via genetic and therapeutic approaches results in reduced mammary tumor growth and even tumor regression (7). Overall, these studies corroborate that TAM play a pivotal role in breast/mammary cancer development, but the underlying molecular mechanisms accounting for the protumor activity of TAM remain unclear.

Macrophages are notoriously heterogeneous, exhibiting functional plasticity in different disease contexts (8, 9). Mirroring Th1/Th2 (T helper cell) polarization, activated macrophages are commonly classified as M1/M2 dichotomy, two extremes in a spectrum of functional states (10, 11). M1 macrophages induced by Th1 cytokines are characterized as having proinflammatory and antitumor activities, whereas M2 macrophages, which are driven by Th2 cytokines, increase angiogenesis and exhibit protumor functions (12). In breast cancer, TAM consist of distinct subpopulations with specialized functions in different tumor regions (13, 14). For example, $Ly6C^{+}$ monocytes can differentiate into $MHCII^{+}CD11c^{+}$ subsets, displaying an M1-like antitumor phenotype in early-stage tumors. In contrast, a great majority of macrophages exhibit an $MHCII^{-}CD11c^{-}$ M2-like protumor phenotype in late stages of tumor development (15). Emerging evidence suggests that different environmental cues or host-produced molecules influence TAM phenotype, skewing them to either a tumor-promoting or a tumor-inhibiting phenotype (16). Therefore, uncovering new factors that are able to shape TAM phenotype and function may lead to novel strategies for breast cancer immunotherapy.

Known as intracellular lipid chaperones facilitating lipid distribution and responses, fatty acid–binding proteins (FABP) are

[1]Department of Microbiology and Immunology, University of Louisville, Louisville, Kentucky. [2]The Hormel Institute, University of Minnesota, Austin, Minnesota. [3]Defense Threat Reduction Agency, Fort Belvoir, Virginia. [4]Minnesota Supercomputing Institute, University of Minnesota, Minneapolis, Minnesota. [5]Gene Analysis Core, Center for Individualized Medicine, Mayo Clinic, Rochester, Minnesota. [6]School of Basic Medical Sciences, Guangzhou Medical University, Guangzhou, China. [7]Department of Bioinformatics and Biostatistics, University of Louisville, Louisville, Kentucky. [8]College of Biological Sciences, University of Minnesota, Minneapolis, Minnesota. [9]Hartford Healthcare Cancer Institute, Hartford, Connecticut.

Note: Supplementary data for this article are available at Cancer Research Online (http://cancerres.aacrjournals.org/).

Corresponding Authors: Bing Li, University of Louisville, 505 South Hancock Street, Louisville, KY 40202. Phone: 502-852-2678; Fax: 502-852-7531; E-mail: b.li@louisville.edu; Jill Suttles, jill.suttles@louisville.edu; and Shujun Liu, The Hormel Institute, University of Minnesota, 801 16th Avenue NE, Austin, MN 55912. Phone: 507-437-9613; Fax: 507-437-9606; E-mail: sliu@hi.umn.edu

doi: 10.1158/0008-5472.CAN-17-2465

key mediators in the regulation of metabolic and inflammatory pathways inside cells (17, 18). We and others have demonstrated that FABPs, in particular epidermal FABP (E-FABP or FABP5) and adipocyte/macrophage FABP (A-FABP or FABP4), play critical roles in various disease models, including metabolic diseases, chronic inflammation, and cancer development (19–21). Interestingly, new evidence from our recent studies suggests that different macrophage subsets have unique FABP expression patterns (19), implying that FABPs may serve as new factors that influence macrophage phenotype and function. In the present study, we report that A-FABP is upregulated in certain subsets of TAM in breast/mammary tumors, which enhances their ability to promote tumor growth and metastasis through IL6–dependent pathways. Thus, A-FABP may serve as a new functional marker for protumor TAM.

Materials and Methods

Mice and human samples

A-FABP WT (*FABP4*$^{+/+}$) mice and A-FABP KO (*FABP4*$^{-/-}$) mice were bred and maintained in the animal facility of the University of Louisville with authorized protocol from the Institutional Animal Care and Use Committee (IACUC). Human samples including normal/benign breast tissues and malignant breast tissues were collected and double-blindly provided by Dr. Edward Sauter. All patients were given written informed consent under an Institutional Review Board–approved protocol in accordance with U.S. Common Rule. Details for tumor cells, syngeneic tumor models are described in the Supplementary Methods.

Prognostic survival and gene-expression analysis

For analyzing the association of FABPs with the overall survival of breast cancer patients, we performed the analysis using PROGgene. See detailed information in the Supplementary Methods.

Macrophage culture and transfection

Both macrophage cell lines and bone marrow–derived macrophages were used in this study. See detailed information of macrophage culture and transfection assays in the Supplementary Methods.

Confocal microscope

Confocal staining was performed to determine A-FABP expression and macrophage infiltration in human breast tumor tissues. See the Supplementary Methods for the details.

Quantitative real-time PCR

Total RNA was extracted using the RNeasy Mini Kit (Qiagen). cDNA synthesis was performed using the QuantiTect Reverse Transcription Kit (Qiagen). The quantitative real-time PCR was carried out with SYBR Green PCR Master Mix on the StepOnePlus Real-Time PCR Systems. For miR-29b expression, qPCR was conducted by TaqMan microRNA assays and normalized by U44/48. Target expression was analyzed using the ΔCT approach. See detailed primer sequences in the Supplementary Table S1.

Flow cytometric analysis

For cell surface staining, immune cells in different organs or in the tumor stroma were stained with anti-CD4 (GK1.5), anti-CD8 (53-6.7), anti-NK1.1 (PK136), anti-CD19 (1D3), anti-F4/80 (BM8), anti-CD11b (M1/70), anti-Ly6C (HK1.4) and anti-MHCII (M5/114.15.2). For intracellular A-FABP staining, cells were stained with anti–A-FABP antibody (MAB3150) after fixation and permeabilization. Cells were acquired by BD FACS Fortessa and BD FACS AriaII Cell Sorter. All the data were analyzed by FlowJo 10.1 as previously described (20).

Colony formation assays

E0771 tumor cell colony formation assay was performed to determine whether A-FABP expression in TAM promotes E0771 colony formation. Details are in the Supplementary Methods.

Western blotting

The procedures of SDS-PAGE and immunoblotting were described as our previous studies (19). Briefly, to measure the expression of target molecules, proteins were acquired from cell lysates and quantified by BCA assay. Anti–mouse-IL6 and anti-NFκB were from Abcam. Anti–A-FABP was from R&D System. Other antibodies, including anti-STAT3, antiphospho-STAT3 (Tyr705), β-actin, GAPDH, were from Cell Signaling Technology.

Reporter gene assays

A total of 5×10^4 293T cells were seeded into 24-well plates for overnight and cotransfected with 2μg of IL6 3-UTR luciferase plasmid (Plasmid #52884, Addgene) with *miR-29b* or its scramble control. pRL-TK *Renilla* luciferase plasmid (Promega) was cotransfected as an internal control. Firefly luciferase activity was measured 48 hours after transfection by using a dual luciferase reporter assay system (Promega) according to the manufacturer's instruction. Values were corrected to account for differences in transfection efficiency by pRL-TK *Renilla* luciferase activity. All luciferase data represent mean±SD of three independent experiments.

ELISA

ELISA kits for mouse IL6, IL10, or TNFα (Biolegend) were used to detect respective cytokines in mouse serum and cell cultural supernatants according to the manufacturer's instruction.

miRNA microarray

miRNA microarray was performed to analyze the miRNA expression profile between WT and A-FABP$^{-/-}$ macrophages. See detailed information in the Supplementary Methods.

Statistical analysis

For analysis of microRNA data, the raw microarray images were imported into Partek Genomics Suite (version 6.6) with a customized normalization method. The cleaned data matrix was then exported to R (version 3.1) and analyzed by Limma packages. The significantly differentially expressed miRNAs were those that showed at least 2-fold change in expression with a false discovery rate (FDR)– corrected *P* value less than 0.05. For other *in vitro* or *in vivo* experiments, a two-tailed, unpaired Student *t* test was performed for the comparison of results. A *P* value of <0.05 is regarded as statistically significant.

Results

Upregulation of A-FABP expression in human breast cancer

To investigate the emerging roles of FABPs in breast cancer, we first analyzed publicly accessible raw databases from Gene

Expression Omnibus (GEO) and The Cancer Genome Atlas using online tool PROGgene to determine whether FABP expression was associated with breast cancer survival. We found that high expression of A-FABP (FABP4), but not other members of FABP family in breast tumor tissues, was significantly associated with low overall survival of total breast cancer patients ($n = 596$), triple-negative patients, and single negative (ER^-, PR^-, or $Her2^-$) patients (Supplementary Fig. S1 and Supplementary Table S2). As A-FABP was primarily expressed in stromal cells, including adipocytes and macrophages, we further analyzed FABP expression pattern in the stroma of breast tissues using GEO dataset GSE9014 (22). We found that A-FABP was the most strongly upreglulated FABP member in breast cancer tissues as compared to normal controls ($P = 3.06E{-}16$; Fig. 1A). Moreover, the upregulation of A-FABP in the stroma was independent of subtypes of breast cancer (Fig. 1B). To verify the potential procancer activity of A-FABP in breast cancer, we analyzed A-FABP expression in benign and malignant breast tissues. Compared with normal/benign breast tissues A-FABP expression was elevated in cancer tissues (Fig. 1C). Significantly more A-FABP positive cells were accumulated in the stroma of malignant tumors regardless of ER status (Fig. 1D). These data strongly suggest that A-FABP may represent a new unappreciated factor in tumor stromal tissues promoting breast cancer progression.

A-FABP deficiency inhibits tumor growth and metastasis

If A-FABP upregulation was able to promote breast cancer progression, we speculated that A-FABP deficiency might inhibit tumor growth and metastasis. To this end, we employed A-FABP deficient ($A\text{-}FABP^{-/-}$) mouse models to assess the impact of A-FABP deficiency on mammary tumor growth and metastasis. Of note, $A\text{-}FABP^{-/-}$ mice developed normally and exhibited similar lipid metabolism, adipokines and immunophenotypes as their WT counterparts under the standard chow diet (Supplementary Fig. S2A–S2F; refs. 23–25). E0771 tumor cells derived from a C57BL/6 mouse mammary adenocarcinoma were

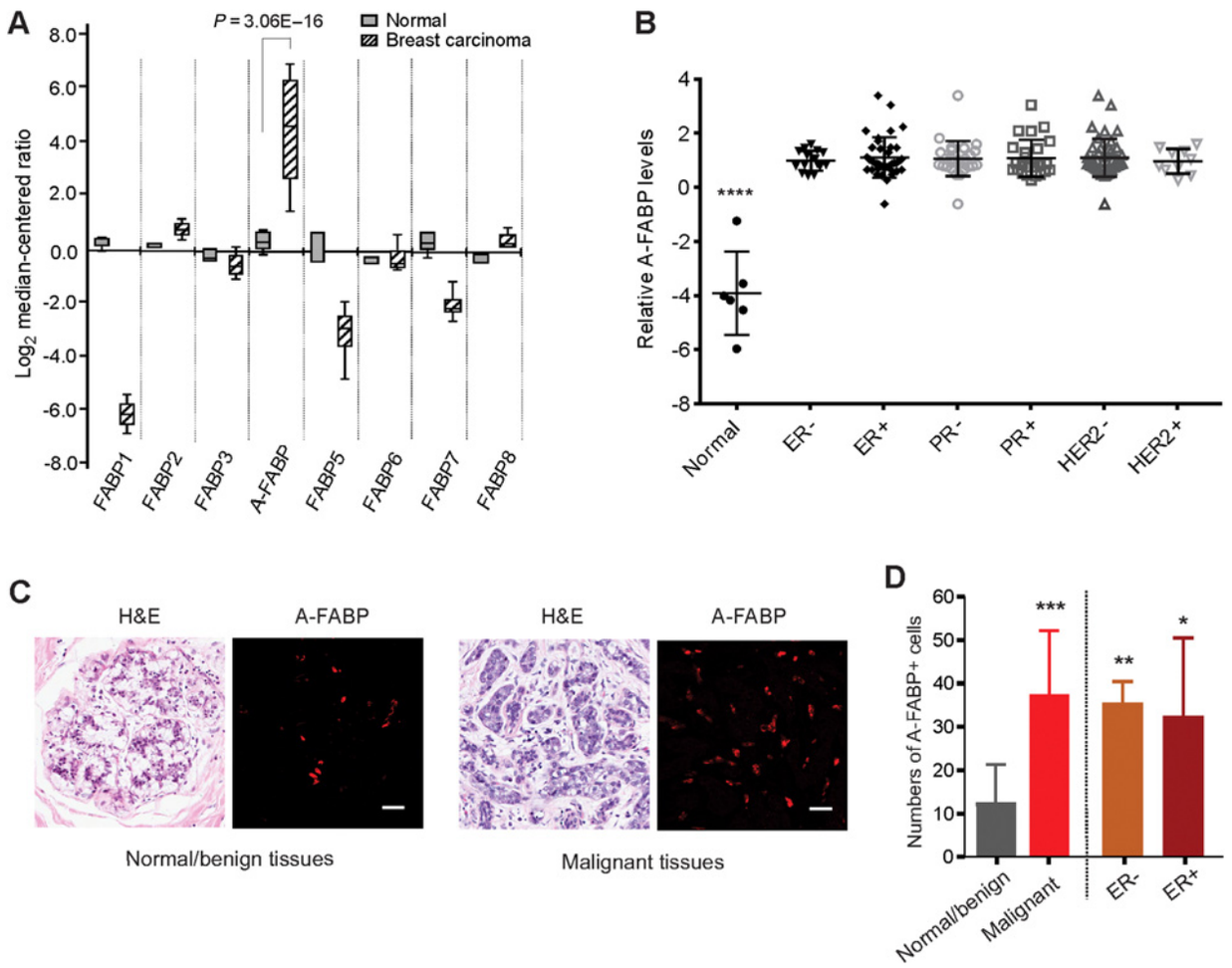

Figure 1.

A-FABP expression is associated with human breast cancer progression. **A** and **B,** Oncomine analysis of the expression pattern of FABP family members in stromal tissues of normal and malignant human breast tissues (**A**) and A-FABP expression in different subtypes of breast cancer (**B**) using the GEO dataset GSE9014. **C,** Hematoxylin and eosin (H&E) staining and confocal analysis of A-FABP expression in normal and malignant human breast tissues; scale bars, 10 μm. **D,** Average numbers of $A\text{-}FABP^+$ cells of the high-power field (×400) in normal/benign ($n = 12$) and malignant ($n = 23$) human breast tissues. *, $P < 0.05$; **, $P < 0.01$; ***, $P < 0.001$ as compared with controls. Data are shown as mean ± SD.

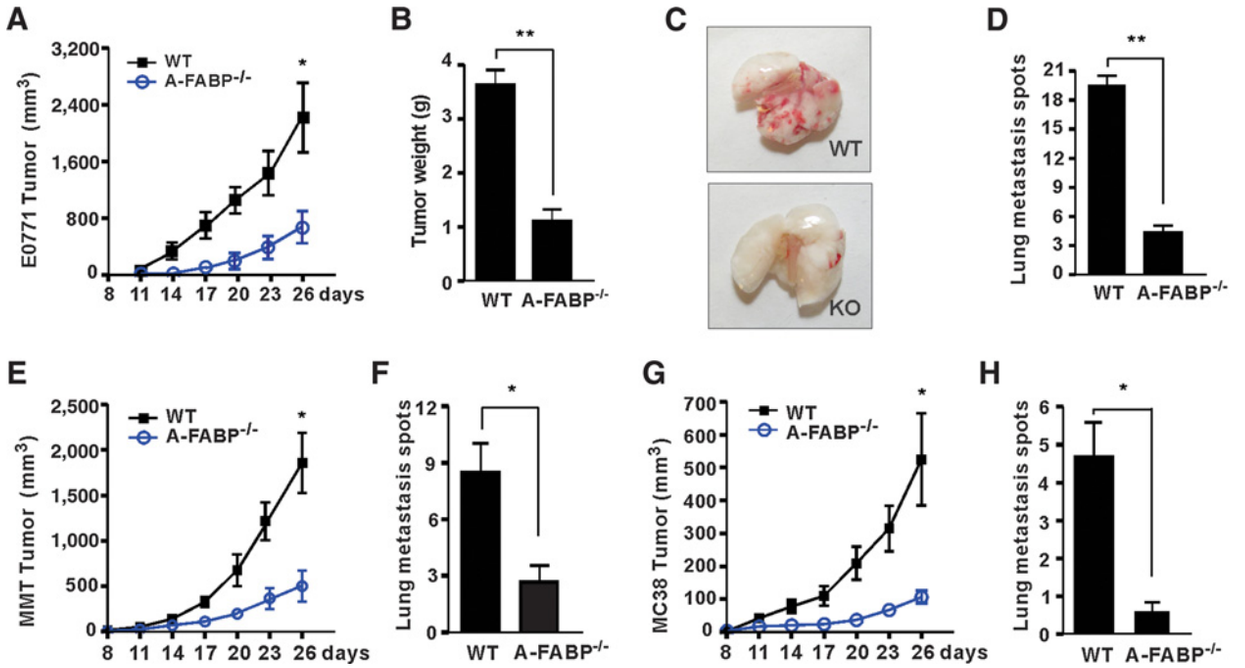

Figure 2.

A-FABP deficiency in mice reduces tumor growth and metastasis. **A,** E0771 mammary tumor cells (1×10^6) were orthotopically injected in the mammary pad of WT and A-FABP$^{-/-}$ mice ($n = 9$/group). Tumor size was measured every 3 days. *, $P < 0.05$; **, $P < 0.01$. **B,** E0771 tumors were removed and weighted on day 26 after tumor implantation from WT and A-FABP$^{-/-}$ mice. **, $P < 0.01$. **C,** Representative pictures of lung metastasis of E0771 tumors in WT and A-FABP$^{-/-}$ mice on day 26 after tumor implantation. **D,** Numbers of lung metastasis spots of E0771 tumors in WT and A-FABP$^{-/-}$ mice on day 26 after tumor implantation. **, $P < 0.01$. **E,** MMT mammary tumor cells (1×10^6) were orthotopically injected in the mammary pad of WT and A-FABP$^{-/-}$ mice ($n = 9$/group). Tumor size was measured every 3 days. *, $P < 0.05$; **, $P < 0.01$. **F,** Numbers of lung metastasis spots of MMT tumors in WT and A-FABP$^{-/-}$ mice on day 26 after tumor implantation. *, $P < 0.05$. **G,** MC38 colon tumor cells (1×10^6) were subcutaneously injected in the flanks of WT and A-FABP$^{-/-}$ mice ($n = 9$/group). Tumor size was measured every 3 days. *, $P < 0.05$; **, $P < 0.01$. **H,** Numbers of lung metastasis spots of MC38 tumors in WT and A-FABP$^{-/-}$ mice on day 26 after tumor implantation. *, $P < 0.05$. Data are shown as mean ± SEM.

orthotopically injected into the mammary fat pad of A-FABP$^{-/-}$ mice and their WT littermates. E0771 tumors grew much slower and average tumor weight was 3-fold less in A-FABP$^{-/-}$ mice than in WT mice (Fig. 2A and B). A-FABP deficiency also significantly reduced E0771 cell-derived lung metastasis (Fig. 2C and D). To determine whether host-derived A-FABP represents a general mechanism for promoting tumor progression, we further evaluated tumor growth and metastasis in WT and A-FABP$^{-/-}$ mice using different types of tumor cells, including mouse mammary tumor cells (MMT) and colon cancer cells (MC38). Similar to the E0771 model, both tumors exhibited significant decrease in tumor growth and lung metastasis when A-FABP was not present in host mice (Fig. 2E–H). Notably, E0771 tumor cells themselves expressed A-FABP whereas the other tested cell lines had low or no A-FABP expression (Supplementary Fig. S2G and S2H). However, regardless of A-FABP expression status in tumor cells, A-FABP deficiency in the host inhibited tumor growth and metastasis. These data collectively suggest that host-derived A-FABP plays a critical role for promoting tumor progression.

A-FABP is upregulated in macrophages that contribute to the enhanced tumor progression

To investigate how A-FABP promotes tumor progression, we first sought to identify which population of stromal cells was responsible for the upregulation of A-FABP expression. In naïve mice without tumors, we evaluated different populations of leukocytes separated from the spleen and found that A-FABP expression was predominantly confined to F4/80$^+$ macrophages (Fig. 3A). Confocal microscopy staining confirmed that A-FABP was expressed in the cytoplasm of bone marrow–derived macrophages from WT mice (Fig. 3B). Interestingly, when macrophages were cultured in the presence of tumor supernatants, A-FABP expression in macrophages was further enhanced (Fig. 3C). By mimicking *in vivo* crosstalk of tumor/macrophages, we cocultured macrophages with tumor cells in Transwell inserts and confirmed that macrophages responded to tumor exposure with elevation of A-FABP expression (Fig. 3D). In contrast, when adipocytes, which also highly expressed A-FABP, were cocultured with tumor cells (Supplementary Fig. S3A), A-FABP expression in adipocytes was downregulated (Supplementary Fig. S3B), suggesting that macrophages, but not adipocytes, are the major populations responsible for the upregulation of A-FABP in the tumor stroma. To substantiate this speculation, macrophages separated from mammary tumors or the spleen of tumor-bearing mice exhibited enhanced expression of A-FABP as compared with those from naïve mice (Fig. 3E). Furthermore, we measured A-FABP expression using surgically-removed benign and malignant human breast tissues and confirmed the elevated expression of A-FABP in CD163$^+$ TAM in patients with invasive breast cancer (Supplementary Fig. S3C). Taken together, our *in vitro* and *in vivo* data suggest that TAM account for the elevated A-FABP expression in the tumor stroma.

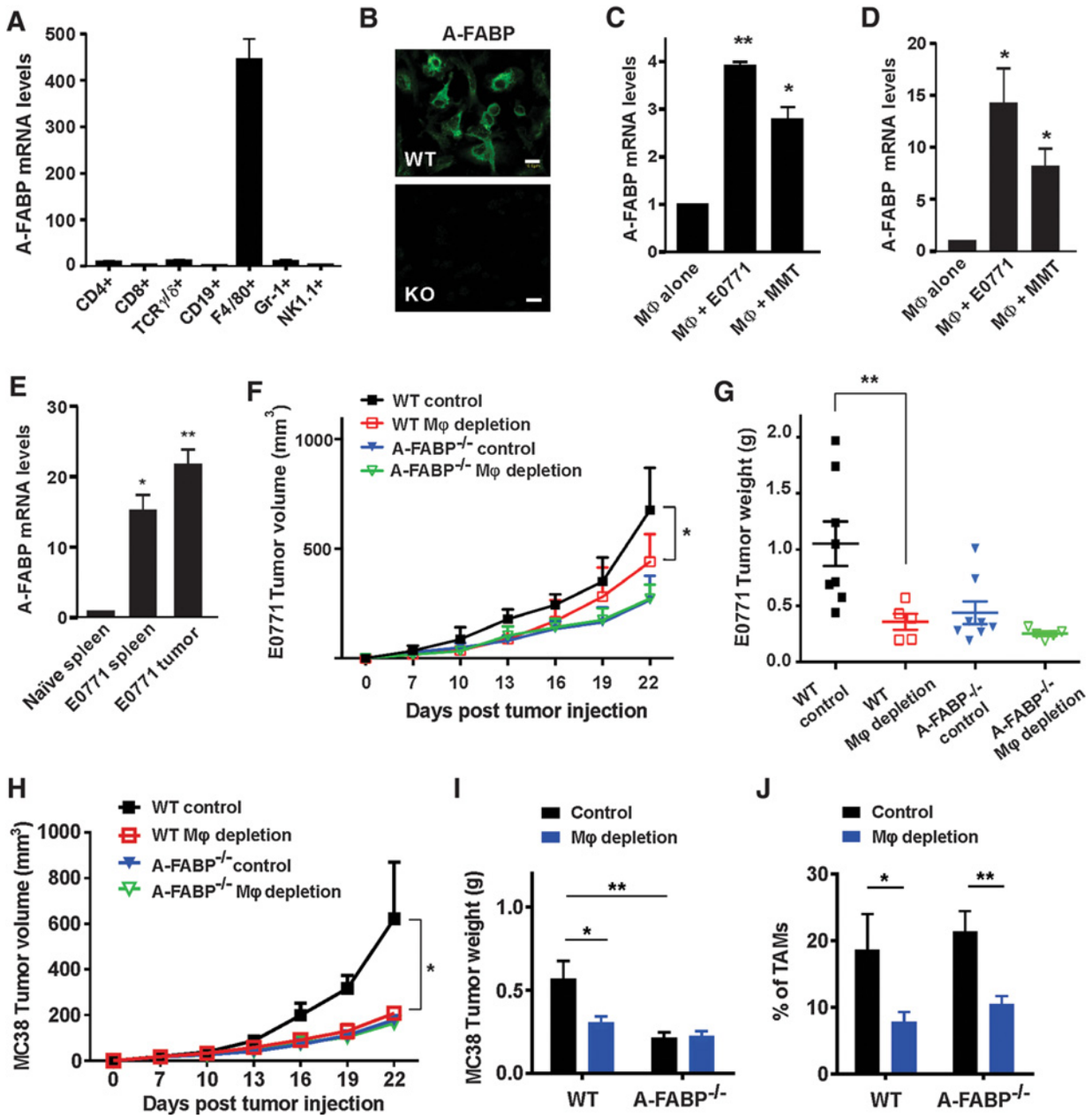

Figure 3.

A-FABP is upregulated in macrophages that contribute to the enhanced tumor progression. **A,** Real-time PCR analysis of A-FABP expression in different subsets of immune cells in spleen. **B,** Confocal staining of A-FABP expression in bone marrow–derived macrophages of WT and A-FABP$^{-/-}$ mice; scale bars, 10 μm. **C,** Real-time PCR analysis of A-FABP expression in bone marrow–derived macrophages stimulated with supernatants collected from E0771 and MMT cells, respectively. *, $P < 0.05$; **, $P < 0.01$. **D,** Bone marrow–derived macrophages were cocultured with indicated tumor cells in a Transwell insert for 24 hours. A-FABP expression in macrophages was analyzed by real-time PCR. *, $P < 0.05$. **E,** Real-time PCR analysis of A-FABP expression in macrophages separated by a flow sorter from the spleen of naive mice and tumor-bearing mice, or from the tumor mass ($n = 3$/group; *, $P < 0.05$; **, $P < 0.01$). **F** and **G,** E0771 tumor cells (0.5×10^6) were orthotopically injected in mice treated with clodronates or control liposomes. Tumor size was measured every 3 days (*, $P < 0.05$; **F**), and E0771 tumors were weighted in WT and A-FABP$^{-/-}$ mice treated with clodronates or control liposomes on day 24 after tumor transplantation (**, $P < 0.01$; **G**). **H** and **I,** MC38 tumor cells (0.5×10^6) were subcutaneously injected in mice treated with clodronates or control liposomes. Tumor size was measured every 3 days (*, $P < 0.05$; **H**), and MC38 tumors were weighted on day 24 after tumor transplantation (*, $P < 0.05$; **, $P < 0.01$; **I**). **J,** Analysis of TAM percentages in MC38 tumor stroma in WT and A-FABP$^{-/-}$ mice with clodronates or control liposomes on day 24 after tumor transplantation. *, $P < 0.05$; **, $P < 0.01$.

Next, we sought to determine whether A-FABP–expressing TAM were responsible for the enhanced tumor growth using clodronate-mediated macrophage depletion assays (26, 27). When mice were intraperitoneally injected with clodronate liposomes or control liposomes, splenic macrophages were successfully depleted in WT and A-FABP$^{-/-}$ mice (Supplementary Fig. S4A). Using this approach, we depleted macrophages in WT and A-FABP$^{-/-}$ mice and measured transplanted tumor growth in these mice. Importantly, macrophage depletion significantly reduced E0771 tumor growth in WT mice, but not in A-FABP$^{-/-}$ mice (Fig. 3F). The marked differences in E0771 tumor weight between WT and A-FABP$^{-/-}$ mice also disappeared after macrophage depletion (Fig. 3G). Consistently, we observed similar results with MC38 tumors after clodronate treatment with significant depletion of TAM in the tumor stroma (Fig. 3H–J). Of note, macrophage depletion with clodronate had no obvious impact on the infiltration of other immune cell populations, including CD8$^+$ T cells, CD4$^+$ T cells, B cells and NK cells, in the tumor stroma (Supplementary Fig. S4B–S4E), suggesting a specific role of macrophages in promoting tumor progression. Altogether, these data indicate that A-FABP is upregulated in macrophages that contribute to tumor progression.

A-FABP is preferentially upregulated in a specific subset of macrophages

Considering the heterogeneous phenotype and function of TAM, we hypothesized that A-FABP might be differentially expressed in different subsets of macrophages. Using high-power confocal microscopy, we observed that A-FABP (red) was expressed in half of the TAM (green) in the tumor stroma of human invasive breast tumor tissues (Fig. 4A). To determine the phenotype of A-FABP$^+$ macrophages, we gated on CD11b$^+$F4/80$^+$ macrophages and identified distinct macrophage subsets using MHCII and Ly6C as markers (Q1 to Q4) in the spleen of naïve WT and A-FABP$^{-/-}$ mice (see gating strategy and FACS definition of Q1 to Q4 in Supplementary Fig. S5A). We separated each subset with a flow sorter and analyzed A-FABP expression levels. We found that A-FABP was preferentially expressed in the Q4 subset of splenic macrophages, which exhibited the F4/80$^+$CD11b$^+$MHCII$^-$Ly6C$^-$ phenotype (Fig. 4B). When we analyzed the peripheral blood using the same gating strategy, monocytes in the blood were divided into two major subsets: Q1 and Q4 (Supplementary Fig. S5B). Consistently, A-FABP was preferentially expressed in the Q4 subset of the peripheral monocytes similar to their counterparts in the spleen (Fig. 4C). When we further analyzed tumor infiltrating macrophage subsets in tumors, about 40% of TAM were located in the Q4 quadrant (Supplementary Fig. S5C). Importantly, A-FABP was also upregulated in this specific subset of TAM (Fig. 4D). Thus, A-FABP seemed to be preferentially expressed in the monocytes/macrophage subset, which exhibited the phenotype of CD11b$^+$F4/80$^+$MHCII$^-$Ly6C$^-$. These results imply that A-FABP may facilitate tumor progression by enhancing the protumor activity of this specific TAM subset.

We next examined the dynamic changes in monocytes/macrophages by focusing on the Q4 subset in tumor-bearing mice over a 3 to 4 weeks period (days 0, 3, 12, and 24 after tumor implantation). We observed that the percentage of the Q4 subset quickly increased in the spleen and blood after tumor cell implantation, and reached peak levels at day 12. However, it decreased dramatically to the basal levels around 4 weeks when mice were sacrificed at the IACUC-required endpoints (Fig. 4E and F). In sharp contrast, the Q4 subset in the tumor stroma increased slowly at the early stage (before day 12), but expanded dramatically at the late stage after tumor cell implantation (Fig. 4G; Supplementary Fig. S5D), suggesting a protumor function of the Q4 subset. To demonstrate that Q4 macrophages were directly involved in promoting mammary tumor growth, we separated splenic Q4 subset from WT and A-FABP$^{-/-}$ mice using a flow sorter, and co-injected with E0771 cells into A-FABP$^{-/-}$ mice, respectively. Strikingly, Q4 macrophages from WT mice, but not A-FABP$^{-/-}$ mice, significantly promoted E0771 tumor growth (Fig. 4H). Tumor size and weight in A-FABP$^{-/-}$ mice coinjected with WT Q4 macrophages were comparable with these of WT mice. In contrast, Q4 macrophages from A-FABP$^{-/-}$ mice had no protumor effect (Fig. 4I and J). All these results indicate that A-FABP is highly expressed in the Q4 macrophage subset, which is accumulated in the tumor stroma directly promoting tumor progression in an A-FABP–dependent manner.

A-FABP functions to promote IL6 production by TAM

To dissect how A-FABP exerts its protumor function in TAM, we separated major TAM subsets from the tumor stroma using a flow sorter as described above (Supplementary Fig. S5C), and analyzed well-known tumor-related molecules produced by TAM. Interestingly, high expression of A-FABP in the Q4 subset of TAM did not impact the expression of well-known markers for M1 and M2, such as iNOS, Arg-1, IL10. and TNFα (Fig. 5A–D), nor did it influence other tumor-related molecules in macrophages, including IL12, CXCR-1, TGFβ, MMP-9, and MMP-1 (Supplementary Fig. S6A–S6E). However, A-FABP$^+$ Q4 TAM exhibited elevated levels of IL6 expression as compared with A-FABP$^{-/-}$ counterparts (Fig. 5E). By measuring circulating levels of cytokines in naïve and tumor-bearing mice, we observed that tumors increased the levels of IL6, but not IL10 and TNFα, in WT mice, but not in A-FABP$^{-/-}$ mice (Fig. 5F–H), suggesting an A-FABP–dependent effect in IL6 upregulation *in vivo*. To verify this effect, we measured IL6 production first by knocking down A-FABP expression with A-FABP shRNA in WT macrophages (Fig. 5I–J), and then by employing A-FABP-deficient macrophages (Fig. 5K–L). Results from both real-time PCR and Western blotting confirmed that IL6 upregulation was controlled by A-FABP expression in macrophages. To further confirm the A-FABP–regulated IL6 production, we analyzed their association using human tumor samples. In the laser-dissected breast cancer stroma samples (GSE9014), we found that A-FABP was significantly positively correlated with IL6 expression (Fig. 5M). This positive correlation was also confirmed in a dataset using whole breast tumor tissues (GSE18229 with 223 breast cancer patients; Supplementary Fig. S6F). All these *in vitro* and *in vivo* evidence indicates that A-FABP controls IL6 production by TAM.

A-FABP regulates IL6 through NFκB–miR-29b pathway

To further investigate the molecular mechanisms by which A-FABP regulates IL6 production in TAM, we conducted miRNA arrays using WT and A-FABP$^{-/-}$ macrophages due to the emerging role of miRs in regulating macrophage function and immune responses in the tumor microenvironment (28, 29). Principal component analysis (PCA) showed that miR clusters of WT macrophages displayed a distinct pattern than that of A-FABP$^{-/-}$ macrophages, suggesting biological differences due to the deficiency of A-FABP (Supplementary Fig. S7A). Heat map

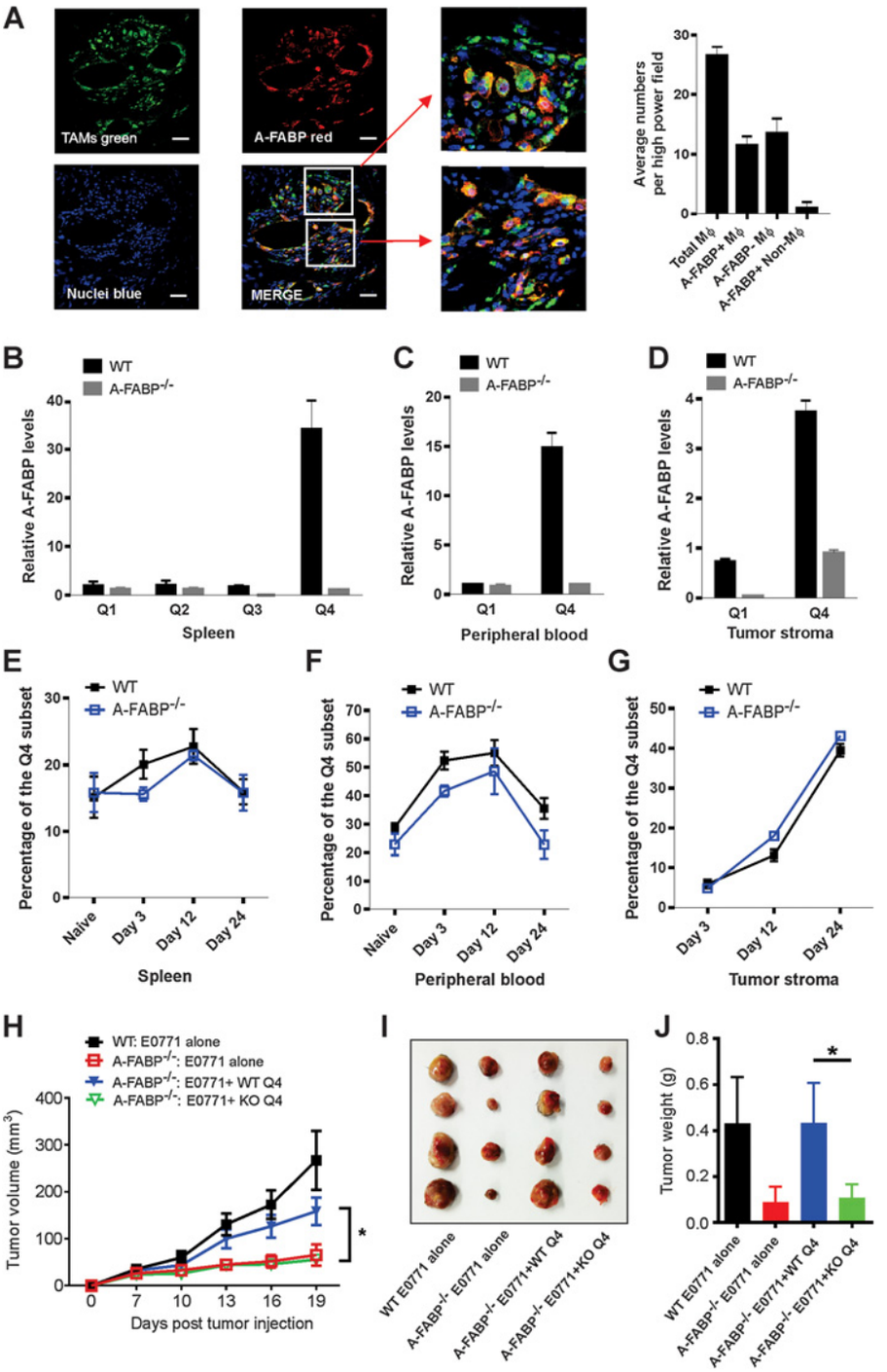

Figure 4.
A-FABP is preferentially expressed in a specific subset of macrophages. **A,** Confocal analysis of A-FABP expression (red) and macrophage infiltration (green) in breast tumor tissues (DAPI for nuclei; $n = 3$). Numbers of total TAM, A-FABP–positive TAM, and A-FABP–negative TAM per high power field are shown in the right panel; scale bars, 10 μm. **B** and **C,** Real-time PCR analysis of A-FABP expression in distinct macrophage subsets separated by a flow sorter from the spleen (**B**), or the peripheral blood (**C**) of naïve WT and A-FABP$^{-/-}$ mice ($n = 3$/group). **D,** Analysis of A-FABP expression by real-time PCR in distinct subsets of tumor-infiltrated macrophages separated by a flow sorter from tumors of WT and A-FABP$^{-/-}$ mice on day 24 after E0771 tumor implantation ($n = 3$/group). **E–G,** Dynamic analysis of the percentage of A-FABP^{+} Q4 subsets in the spleen (**E**), the peripheral blood (**F**), and the tumor stroma (**G**) of WT and A-FABP$^{-/-}$ mice ($n = 3$/group) by real-time PCR at the indicated time points after tumor implantation. **H,** Tumor growth curve of E0771 (5×10^5) mixed with or without splenic Q4 subset of macrophages (1×10^5) purified from WT and A-FABP$^{-/-}$ mice ($n = 4$/group; *, $P < 0.05$). **I** and **J,** Tumor size (**I**) and weight (**J**) of E0771 tumors on 21 days post tumor injection in WT and A-FABP$^{-/-}$ mice. *, $P < 0.05$.

analysis identified a group of miRs that were differentially expressed between WT and A-FABP$^{-/-}$ macrophages (Supplementary Fig. S7B). Among them, upregulation of *miR-29b* in A-FABP$^{-/-}$ macrophages (Fig. 6A) particularly attracted our attention as our previous studies have shown that A-FABP enhances activation of NFκB, which negatively regulates *miR-29b* expression (30, 31). We thus speculated that A-FABP may regulate tumor-promoting IL6 production through the NFκB/*miR29b* pathway in macrophages. To this end, we first demonstrated that A-FABP deficiency significantly impaired tumor-stimulated NFκB activation in macrophages (Fig. 6B). Using real-time PCR, we next confirmed that *miR-29b* was indeed elevated when A-FABP was either transiently or stably knocked down in macrophages (Fig. 6C and D). Importantly, when macrophages were transfected

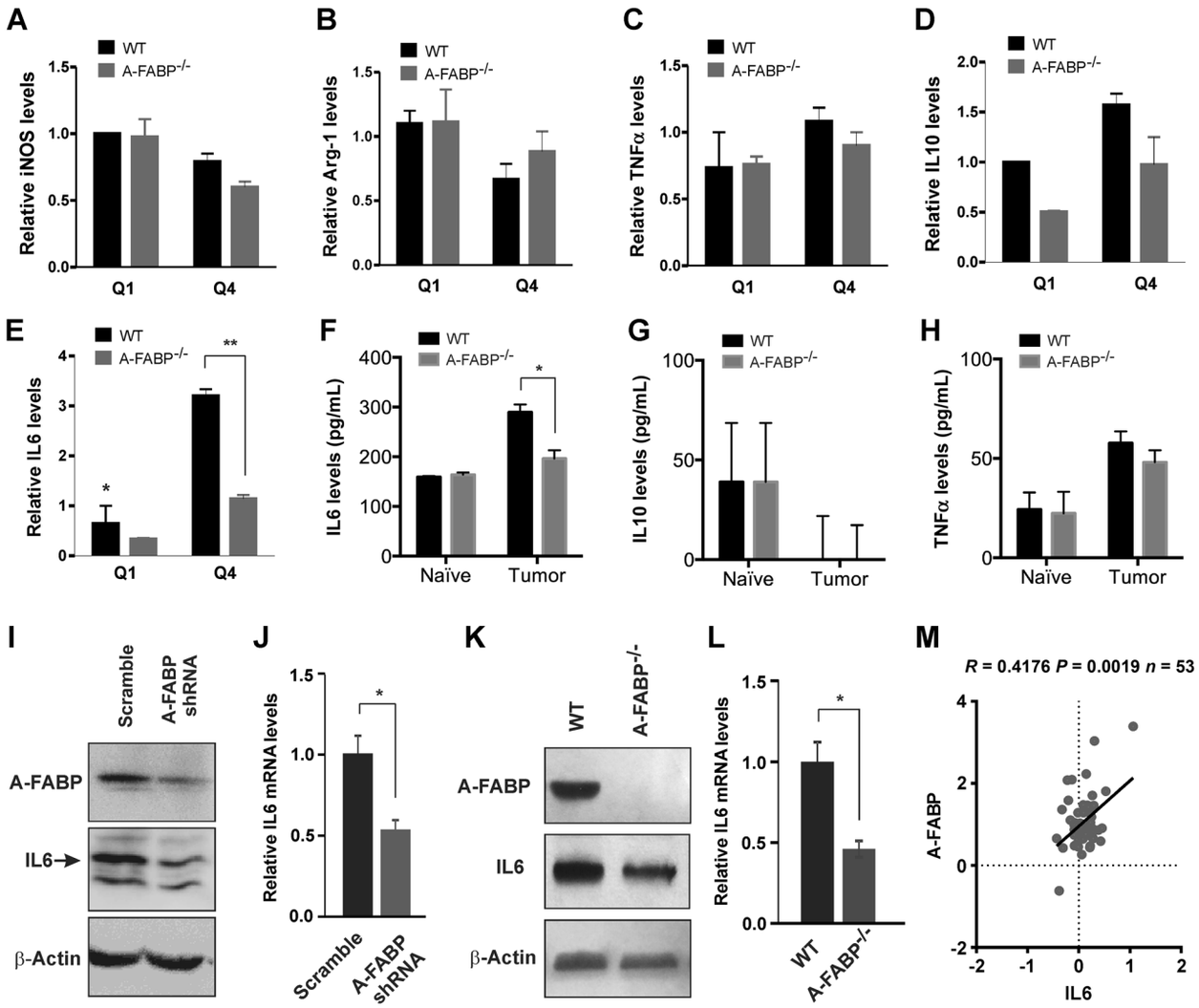

Figure 5.

Expression of A-FABP in macrophages promotes IL6 production. **A–E,** Analysis of the expression of iNOS (**A**), Arg-1 (**B**), TNFα (**C**), IL10 (**D**), and IL6 (**E**) in major subsets of TAM separated from the tumor stroma of WT and A-FABP$^{-/-}$ mice on day 26 after tumor implantation ($n = 3$/group) by real-time PCR. **, $P < 0.01$. **F–H,** Measurements of IL6 (**F**), IL10 (**G**), and TNFα (**H**) in the serum of naïve mice or E0771 tumor-bearing mice sacrificed on day 26 after tumor implantation by ELISA ($n = 3$/group; *, $P < 0.05$). **I** and **J,** Analysis of IL6 expression by Western blotting (**I**) and real-time PCR (**J**) in the WT macrophage cell line transfected with scramble shRNA or A-FABP–specific shRNA. *, $P < 0.05$. **K** and **L,** Analysis of IL6 expression by Western blotting (**K**) and real-time PCR (**L**) in WT and A-FABP$^{-/-}$ macrophage cell lines. *, $P < 0.05$. **M,** Correlation analysis of A-FABP and IL6 in GEO dataset GSE9014. Statistical significance was calculated using Spearman correlation.

with NFκB p65 shRNA (Fig. 6E), knocking down of NFκB not only enhanced *miR-29b* expression (Fig. 6F), but also inhibited IL6 production at both mRNA and protein levels (Fig. 6G and H). Considering that miRs negatively regulate target gene expression through direct binding to their 3′UTR regions, we identified a target sequence on IL6 3′UTR (414-420), which paired with *miR-29b* using the miR target prediction algorithm TargetScan. To validate the direct regulation of *miR-29b* binding to IL6 3′UTR, we cotransfected 293T cells with IL6-3′UTR luciferase plasmid and *miR-29b* or scramble controls, and demonstrated that *miR-29b* was able to significantly reduce IL6 3′UTR luciferase activity as compared with the scramble control (Fig. 6I). Moreover, when *miR-29b* was overexpressed in macrophages (Fig. 6J), IL6 production was significantly inhibited at both mRNA and protein levels (Fig. 6K and L). The negative association of A-FABP with *miR-29b* expression was further verified in human breast cancer samples when we analyzed a well-annotated cohort of 207 breast cancer patients with matched mRNA and microRNA expression profile (GEO dataset: GSE22220; $P < 0.0001$; Supplementary Fig. S7C). In addition, we found that higher *miR-29b* expression was positively associated with better breast cancer survival probability in this dataset (Supplementary Fig. S7D), which further supports the functional role of the A-FABP/*miR-29b* pathway in human breast cancer patients. Collectively, all these data suggest that A-FABP regulates IL6 production, at least partially, via the NFκB/*miR-29b* pathway in macrophages.

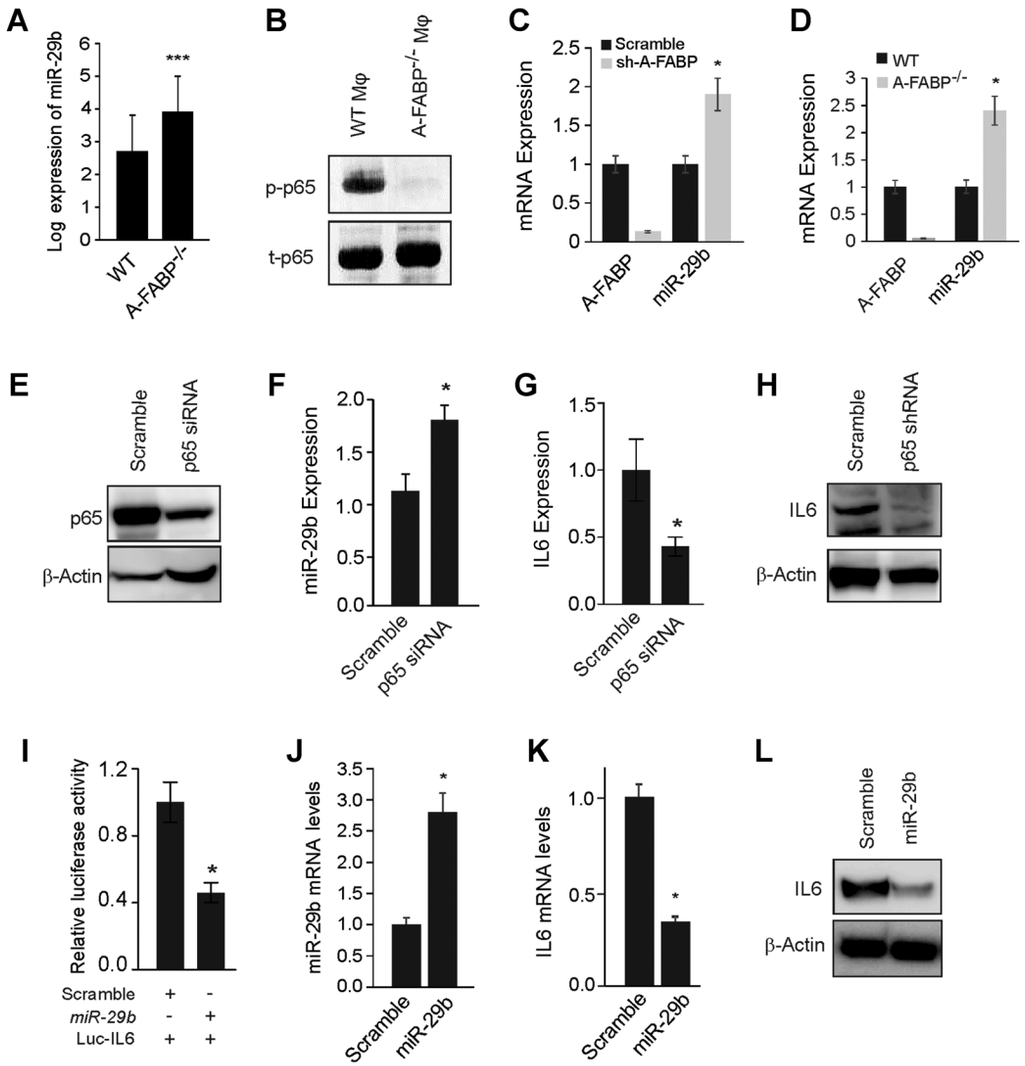

Figure 6.

A-FABP promotes IL6 production via the NFκB/*miR-29b* pathway in macrophages. **A,** Quantification of *miR-29b* expression in primary WT and A-FABP$^{-/-}$ macrophages by miR array analysis. ***, FDR-corrected $P < 0.001$. **B,** Analysis of phospho- and total NFκB p65 in WT and A-FABP$^{-/-}$ macrophage cell lines by Western blotting. **C,** Real-time PCR analysis of A-FABP and *miR-29b* expression in the WT macrophage cell line transfected with scramble or A-FABP shRNA. *, $P < 0.05$. **D,** Analyzing the expression of A-FABP and *miR-29b* in WT and A-FABP$^{-/-}$ macrophage cell lines by real-time PCR. *, $P < 0.05$. **E,** Analysis of NFκB p65 expression in macrophage cell line transfected with scramble or p65 siRNA by Western blotting. **F,** Analysis of *miR-29b* expression in the macrophage cell line transfected with scramble or NFκB p65 siRNA by real-time PCR. *, $P < 0.05$. **G–H,** Analysis of IL6 expression by real-time PCR (**G**) and Western blotting (**H**) in the macrophage cell line transfected with scramble or NFκB p65 siRNA. *, $P < 0.05$. **I,** Analysis of relative luciferase activity of IL6 3′-UTR in 293T cells cotransfected with miR-29b or scramble control by dual luciferase reporter assays. *, $P < 0.05$. **J,** Real-time PCR analysis of *miR-29b* expression in the macrophage cell line transfected with scramble or synthetic *miR-29b* oligos. *, $P < 0.05$. **K–L,** Analysis of IL6 expression by real-time PCR (**K**) and Western blotting (**L**) in the macrophage cell line transfected with scramble or synthetic *miR-29b* oligos. *, $P < 0.05$. Data are shown as mean ± SD and are representative of three experiments.

A-FABP^{+} TAM induces tumorigenic signaling and promotes tumor progression

Considering the well-characterized pathway of IL6/STAT3 in promoting tumor growth and metastasis (32, 33), we next determined whether A-FABP^{+} macrophages promote tumor cell invasiveness by focusing on IL6/STAT3 signaling. When E0771 tumor cells were cocultured with A-FABP^{+} WT or A-FABP$^{-/-}$ macrophages, respectively, we observed that WT macrophages, but not A-FABP$^{-/-}$ macrophages, greatly induced STAT3 phosphorylation in E0771 cells (Fig. 7A). Of note, STAT3 phosphorylation could be blocked by anti–IL6–neutralizing antibody, suggesting that TAM activate tumor cells through A-FABP-dependent IL6/STAT3 signaling. Moreover, we performed tumor-colony formation assays as further verification of the protumor function of A-FABP^{+} TAM. As shown in Fig. 7B and C, macrophage expression of A-FABP significantly promoted tumor colony formation, which was able to be blocked by anti-IL6–neutralizing antibody. As *miR-29b* inhibited IL6 production in macrophages, we cocultured E0771 tumor cells with *miR-29b*- or scramble-transfected macrophages and showed

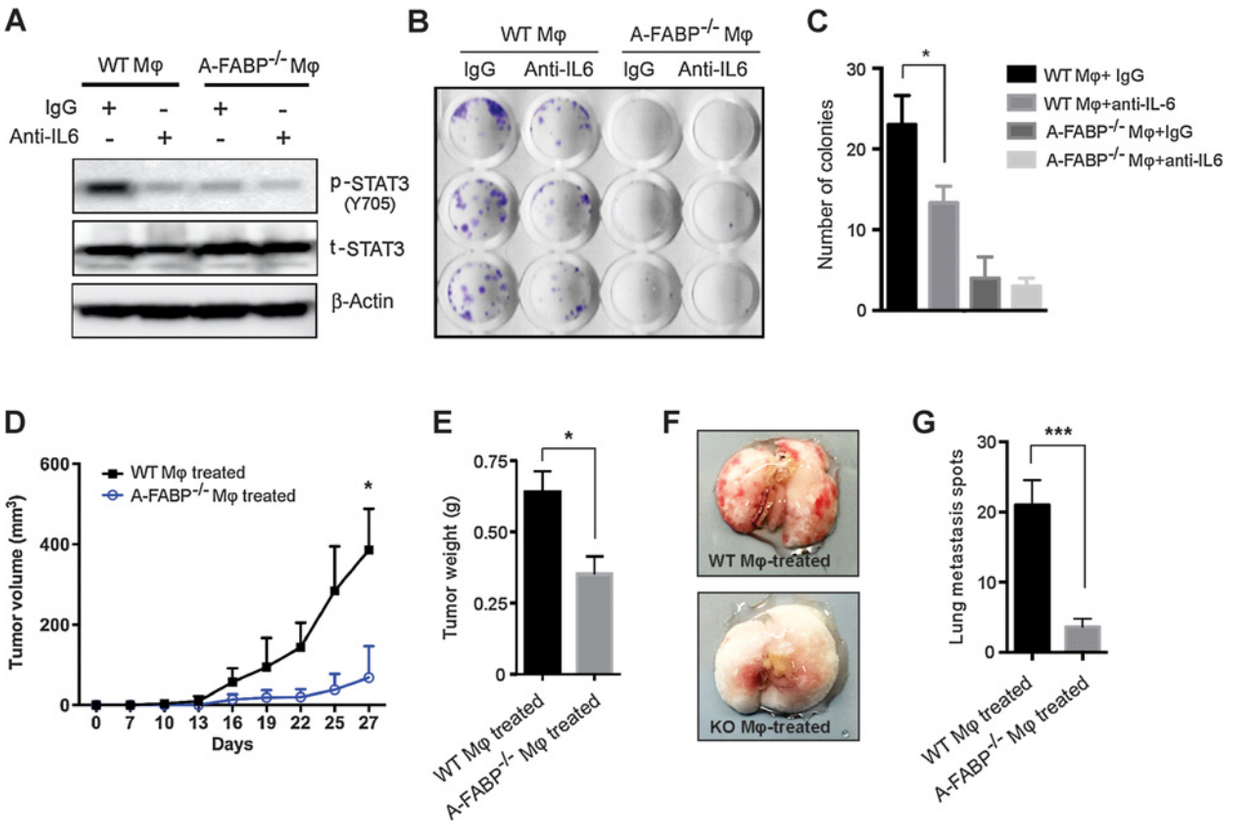

Figure 7.

A-FABP$^+$ TAM induces tumorigenic signaling and promotes tumor progression. **A,** Western blotting for phospho-STAT3 (Y705) and total-STAT3 in E0771 cells stimulated with supernatants of WT and A-FABP$^{-/-}$ macrophage cell lines in the presence or absence of anti-IL6–neutralizing mAb. β-Actin was measured as a loading control. **B** and **C,** Colony formation assays of E0771 tumor cells stimulated with supernatants of WT and A-FABP$^{-/-}$ macrophage cell lines in the presence or absence of anti-IL6–neutralizing mAb. Number of colonies in each group is shown in **C**. *, $P < 0.05$. **D–G,** E0771 tumor cells were cocultured with supernatants of WT- or A-FABP$^{-/-}$ macrophage cell lines for 12 hours and 0.5×10^6 cells were orthotopically injected in C57BL/6 mice ($n = 5$/group). **D,** Tumor size was measured every 3 days. Mice were sacrificed on day 27 after implantation for analyses of tumor weight (**E**) and lung metastasis. Representative pictures of lung metastasis (**F**) and average tumor metastatic spots (**G**) in the lungs of above mice. *, $P < 0.05$; ***, $P < 0.001$.

that *miR-29b*-transfected macrophages significantly reduced STAT3 phosphorylation and colony formation of E0771 cells when compared with scramble controls (Supplementary Fig. S8A–S8C), also confirming the functional role of A-FABP/*miR-29b*/IL6 signaling in enhancing the invasiveness of tumor cells *in vitro*.

To further test protumor function of A-FABP$^+$ macrophages *in vivo*, we cocultured E0771 tumor cells with either A-FABP$^+$ or A-FABP$^-$ macrophages, and respectively implanted them into the mammary fat pads of mice for observation of tumor growth and metastasis. Indeed, tumor cells conditioned with A-FABP$^+$ macrophages grew much faster than those conditioned with A-FABP$^-$ macrophages (Fig. 7D and E). In addition, tumor cells treated with A-FABP$^+$ macrophages showed enhanced capability to metastasize to the lung as compared to these treated with A-FABP$^-$ macrophages (Fig. 7F and G; $P < 0.001$). As E0771 tumor cells, but not host cells from lung tissues, exhibited unique a CD44$^+$CD24$^-$ phenotype (Supplementary Fig. S8D–S8E), we also quantitatively analyzed CD44$^+$CD24$^-$ tumor cells metastasizing to lung tissues by flow cytometric staining. The data clearly showed that A-FABP depletion significantly decreased tumor growth and metastatic spread (Supplementary Fig. S8F–S8G). Taken together, our data confirmed that A-FABP expression in macrophages is critical for tumorigenic signaling, and tumor progression, thereby establishing the protumor function of A-FABP in macrophages.

Discussion

Cancer immunotherapy, in particular macrophage-directed immunotherapy, has been proposed as a breakthrough strategy for eliminating cancer (34). However, due to the complexity of macrophage biology, uncovering novel cellular and molecular mechanisms determining TAM phenotype and function will be critical for translation of these seminal ideas into the clinical setting. Herein, we identified A-FABP as a new tumor-promoting factor in the context of breast cancer. Breast stromal levels of A-FABP were similar among different subtypes of breast cancer, but significantly higher than noncancer controls, suggesting that A-FABP upregulation in tumor stroma represents a general mechanism of protumor effects regardless of subtypes of breast cancer.

Most importantly, we demonstrated that A-FABP promoted tumor progression via enhancing the protumor activity of TAM, specifically within a subset of TAM that exhibit a $CD11b^+F4/80^+Ly6C^-MHCII^-CD11c^-$ phenotype. Mechanistically, A-FABP expression in TAM facilitated the protumor IL6/STAT3 signaling through regulation of the NFκB/*miR-29b* pathway. Thus, the current study not only establishes A-FABP as a new marker for protumor macrophages, but also increases our mechanistic understanding of several important aspects of macrophage-based tumor immunotherapy.

TAMs are notoriously heterogeneous exhibiting both anti- and protumor activities. However, the identification of functional subsets has been challenging. Although the classical M1/M2 dichotomy has served as a model of macrophage function, the *in vivo* setting is very complex due to functional overlap and lack of specificity. For example, Arginase I, usually classified as a M2 marker since it converts arginine to tumor-promoting ornithine, is also upregulated in LPS/IFNγ-stimulated M1 macrophages (35). Through analysis of publicly accessible databases, we found that high expression of A-FABP in human breast tumor tissues was significantly associated with a lower survival rate of breast cancer patients. Mice deficient for A-FABP exhibited reduced tumor growth and metastasis as compared with their WT littermates. Macrophages and adipocytes are the two main populations that highly express A-FABP. Our data demonstrated that A-FABP upregulation in tumor was primarily restricted to a subset of TAM, but not in adipocytes in the tumor stroma. Using clodronate-mediated macrophage depletion assay we showed that macrophage expression of A-FABP was key to their protumorigenic effect. Phenotypically, A-FABP was highly expressed in the Q4 subset of monocytes/macrophages in both mice and humans. Functionally, A-FABP$^+$ TAM separated from mammary tumors exhibited enhanced production of tumor-promoting molecules (e.g., IL6) as compared with A-FABP$^{-/-}$ TAM. Moreover, we further showed that A-FABP expression in macrophages was critical for tumorigenic signaling and colony formation of mammary tumor cells *in vitro* and their growth and metastasis *in vivo*. Thus, our data suggest that A-FABP may serve as a new functional marker for protumor macrophages.

As the most abundant stromal cells in breast/mammary tumors, TAM account for up to 50% of the cells in the tumor mass (36, 37). The question remains as to how TAMs are dynamically regulated during tumor development. Although mounting evidence suggests that TAM originate primarily from bone marrow-derived circulating monocytes (38, 39), the factors controlling the dynamic changes in heterogeneous subsets of TAM in the tumor stroma remain unclear. Most circulatory mouse monocytes are $CD11b^+F4/80^+MHCII^-Ly6C^+$ inflammatory monocytes (Q1 subset) and $CD11b^+F4/80^+MHCII^-Ly6C^-$ patrolling monocytes (Q4 subset). Although published studies have shown that $Ly6C^+$ monocytes are able to differentiate into different subsets of macrophages in tumor models and in muscle injury (15, 40), distinct populations of macrophages in inflammatory tissues can also be sequentially mobilized from the circulation with recruitment of $Ly6C^+$ monocytes in the early stage, whereas $Ly6C^-$ monocytes appear in the late stage (41, 42). Our data showed that A-FABP was preferentially expressed in $CD11b^+F4/80^+MHCII^-Ly6C^-$ macrophages (Q4 subsets) in different tissues, including the spleen, PBMCs, and tumors. By dynamic analysis of macrophage phenotypes in syngeneic mouse models, our previous and current studies demonstrated that macrophages, which were recruited in the tumor stroma in the early stages (1 week after tumor implantation), mainly exhibited a $CD11b^+F4/80^+Ly6C^+$ phenotype with high expression of E-FABP and exerted antitumor function. In contrast, macrophages that accumulated in the late stage of tumors (2–4 weeks after tumor implantation) exhibited a $CD11b^+F4/80^+MHCII^-Ly6C^-$ phenotype with high levels of A-FABP expression and promoted tumor growth and metastasis. In addition, the dynamic changes in macrophage phenotype within the tumor stroma corresponded well to the changes of circulating monocytes in the peripheral tissues, suggesting that TAM could also be recruited from monocytes in the periphery. In addition, we also found that A-FABP is highly expressed in the $CD14^{dim}CD16^+$ monocytes in humans. Thus, measuring A-FABP$^+$ monocytes/macrophages in peripheral blood may provide new evidence for the evaluation of tumor progression in the early stages of tumor development.

How do TAM exert their pro- or antitumor activity? In syngeneic mouse models, we noticed that mammary tumor formation was critical in the first week after tumor cell implantation. Once tumors were established, tumor cells exhibited exponential growth. Indeed, early-infiltrating TAM have been shown to exhibit antitumor activity through E-FABP–mediated type I IFNβ responses (19). In the current study, we noticed that significant tumor growth differences began around 2 weeks (14–17 day) after tumor implantation between WT and A-FABP$^{-/-}$ mice. Moreover, TAM at these stages supported tumor progression by upregulation of A-FABP, which promoted tumor growth via IL6/STAT3 signaling. In line with our observations, the tropic role of A-FABP in promoting tumor growth was confirmed in other models (43, 44). Of note, FABPs constitute a family of 9 proteins with different patterns of tissue distribution. Members of FABPs are traditionally thought to exhibit similar functions via transporting fatty acids and coordinate lipid responses inside cells. However, our research demonstrated an unexpected but novel finding that suggests opposing roles of individual FABPs in regulating macrophage phenotype and function in the tumor setting. Simply put, E-FABP expressed in a subset of $CD11b^+F4/80^+MHCII^+Ly6C^+$ macrophages enhances their antitumor function, whereas A-FABP expressed in a subset of $CD11b^+F4/80^+MHCII^-Ly6C^-$ macrophages facilitates their protumor function.

Mounting evidence suggests an important role of miRs in regulating immune responses and tumor development and progression. Among them, *miR-29b* has been shown to act as a tumor suppressor in many types of cancer including breast cancer (45, 46). Through direct inhibition of oncogenic genes, such as STAT3 and cyclin-dependent protein kinase 6, in tumor cells, *miR-29b* can greatly inhibit tumor growth (45, 47). Moreover, macrophages transfected with *miR-29b* is associated with M1-associated transcripts (29). These studies suggest a beneficial effect of *miR-29b* in inhibiting tumor progression by targeting both tumor cells and immune cells. In the current studies, we demonstrated for the first time that expression of A-FABP in macrophages downregulated *miR-29b* through enhanced NFκB activity, which substantiated our previous observation that activation of NFκB repressed *miR-29b* expression in leukemia cells (30). We further showed that upregulated *miR-29b* in A-FABP$^{-/-}$ macrophages was responsible for the inhibition of IL6/STAT3 signaling and subsequent tumor colony formation, providing a molecular mechanism by which A-FABP promotes the protumor activity of TAM through regulation of the *miR-29b*/IL6 axis.

Targeting TAM for tumor immunotherapy has been proposed as a promising clinical treatment (34, 48), but this has been difficult to achieve in practice due to the heterogeneous and dynamic nature of macrophages in the tumor environment. For example, strategies of either blocking TAM recruitment or depleting TAM and their progenitors have not proven clinically feasible (49). Considering that TAM can exhibit both pro- and antitumor activity depending on different disease settings, identification of functional subsets is key for the design of effective immunotherapies. In the current study, we identified A-FABP as a functional marker for protumor TAM. Thus, inhibition of A-FABP may offer a novel strategy for cancer treatment by specifically targeting tumor-promoting TAM. Indeed, inhibition of A-FABP activity through small-molecule inhibitors has been shown effective in treatment of diabetes and atherosclerosis. It will be of great interest to test their therapeutic efficacy in the treatment of breast cancer.

In summary, our studies suggest A-FABP as a new predictor for breast cancer progression through enhancement of the protumor activity of TAM. Specifically, A-FABP is preferentially expressed in a subset of macrophages ($CD11b^+F4/80^+MHCII^-Ly6C^-$) that are directly involved in promoting tumor growth. Mechanistically, this macrophage subset accumulated in the tumor stroma enhances tumor progression through A-FABP–mediated *miR-29b*/IL6/STAT3 cascade (Supplementary Fig. S9). Thus, A-FABP may serve as a new functional marker for protumor TAM, and targeting A-FABP$^+$ TAM may represent a novel strategy for tumor immunotherapy.

Disclosure of Potential Conflicts of Interest

No potential conflicts of interest were disclosed.

Authors' Contributions

Conception and design: A. Triplett, D.A. Bernlohr, M.P. Cleary, J. Suttles, B. Li
Development of methodology: J. Hao, F. Yan, Y. Zhang, B. Li
Acquisition of data (provided animals, acquired and managed patients, provided facilities, etc.): J. Hao, Y. Zhang, Y. Sun, J. Zeng, E. Sauter
Analysis and interpretation of data (e.g., statistical analysis, biostatistics, computational analysis): J. Hao, F. Yan, A. Triplett, Y. Zhang, K.A.T. Silverstein, Q. Zheng, E. Sauter, B. Li
Writing, review, and/or revision of the manuscript: J. Hao, K.A.T. Silverstein, D.A. Bernlohr, M.P. Cleary, N.K. Egilmez, E. Sauter, S. Liu, J. Suttles, B. Li
Administrative, technical, or material support (i.e., reporting or organizing data, constructing databases): J. Hao, Y. Sun, S. Liu, B. Li
Study supervision: S. Liu, B. Li
Other (processed the samples and provided the resulting data for analysis): D.A. Schultz

Acknowledgments

The authors thank the Mayo Clinic Genome Analysis Core for the help with performing microRNA expression array of macrophages and Minnesota Supercomputing Institute for computing resources used for the microarray analysis. This work was supported by NIH R01 grants CA18098601A1 (to B. Li), CA17767901A1 (to B. Li), and AI048850 (to J. Suttles).

The costs of publication of this article were defrayed in part by the payment of page charges. This article must therefore be hereby marked *advertisement* in accordance with 18 U.S.C. Section 1734 solely to indicate this fact.

Received August 15, 2017; revised December 25, 2017; accepted February 2, 2018; published first February 6, 2018.

References

1. Forouzanfar MH, Foreman KJ, Delossantos AM, Lozano R, Lopez AD, Murray CJ, et al. Breast and cervical cancer in 187 countries between 1980 and 2010: a systematic analysis. Lancet 2011;378:1461–84.
2. Siegel RL, Miller KD, Jemal A. Cancer statistics, 2016. CA Cancer J Clin 2016;66:7–30.
3. Valastyan S, Weinberg RA. Tumor metastasis: molecular insights and evolving paradigms. Cell 2011;147:275–92.
4. Kessenbrock K, Plaks V, Werb Z. Matrix metalloproteinases: regulators of the tumor microenvironment. Cell 2010;141:52–67.
5. Robinson BD, Sica GL, Liu YF, Rohan TE, Gertler FB, Condeelis JS, et al. Tumor microenvironment of metastasis in human breast carcinoma: a potential prognostic marker linked to hematogenous dissemination. Clin Cancer Res 2009;15:2433–41.
6. Condeelis J, Pollard JW. Macrophages: obligate partners for tumor cell migration, invasion, and metastasis. Cell 2006;124:263–6.
7. Lin EY, Nguyen AV, Russell RG, Pollard JW. Colony-stimulating factor 1 promotes progression of mammary tumors to malignancy. J Exp Med 2001;193:727–40.
8. Gordon S, Taylor PR. Monocyte and macrophage heterogeneity. Nat Rev Immunol 2005;5:953–64.
9. Stout RD, Jiang C, Matta B, Tietzel I, Watkins SK, Suttles J. Macrophages sequentially change their functional phenotype in response to changes in microenvironmental influences. J Immunol 2005;175:342–9.
10. Martinez FO, Helming L, Gordon S. Alternative activation of macrophages: an immunologic functional perspective. Annu Rev Immunol 2009;27:451–83.
11. Mosser DM, Edwards JP. Exploring the full spectrum of macrophage activation. Nat Rev Immunol 2008;8:958–69.
12. Mantovani A, Sica A. Macrophages, innate immunity and cancer: balance, tolerance, and diversity. Curr Opin Immunol 2010;22:231–7.
13. Laoui D, Movahedi K, Van OE, Van den Bossche J, Schouppe E, Mommer C, et al. Tumor-associated macrophages in breast cancer: distinct subsets, distinct functions. Int J Dev Biol 2011;55:861–7.
14. Lewis CE, Pollard JW. Distinct role of macrophages in different tumor microenvironments. Cancer Res 2006;66:605–12.
15. Movahedi K, Laoui D, Gysemans C, Baeten M, Stange G, Van den Bossche J, et al. Different tumor microenvironments contain functionally distinct subsets of macrophages derived from Ly6C(high) monocytes. Cancer Res 2010;70:5728–39.
16. Rolny C, Mazzone M, Tugues S, Laoui D, Johansson I, Coulon C, et al. HRG inhibits tumor growth and metastasis by inducing macrophage polarization and vessel normalization through downregulation of PlGF. Cancer Cell 2011;19:31–44.
17. Furuhashi M, Hotamisligil GS. Fatty acid-binding proteins: role in metabolic diseases and potential as drug targets. Nat Rev Drug Discov 2008;7:489–503.
18. Storch J, Corsico B. The emerging functions and mechanisms of mammalian fatty acid-binding proteins. Annu Rev Nutr 2008;28:73–95.
19. Zhang Y, Sun Y, Rao E, Yan F, Li Q, Zhang Y, et al. Fatty acid binding protein E-FABP restricts tumor growth by promoting IFNbeta responses in tumor-associated macrophages. Cancer Res 2014;74:2986–98.
20. Zhang Y, Li Q, Rao E, Sun Y, Grossmann ME, Morris RJ, et al. Epidermal fatty acid binding protein promotes skin inflammation induced by high-fat diet. Immunity 2015;42:953–64.
21. Makowski L, Boord JB, Maeda K, Babaev VR, Uysal KT, Morgan MA, et al. Lack of macrophage fatty-acid-binding protein aP2 protects mice deficient in apolipoprotein E against atherosclerosis. Nat Med 2001;7:699–705.
22. Finak G, Bertos N, Pepin F, Sadekova S, Souleimanova M, Zhao H, et al. Stromal gene expression predicts clinical outcome in breast cancer. Nat Med 2008;14:518–27.
23. Baar RA, Dingfelder CS, Smith LA, Bernlohr DA, Wu C, Lange AJ, et al. Investigation of in vivo fatty acid metabolism in AFABP/aP2(-/-) mice. Am J Physiol Endocrinol Metab 2005;288:E187–E193.
24. Hertzel AV, Smith LA, Berg AH, Cline GW, Shulman GI, Scherer PE, et al. Lipid metabolism and adipokine levels in fatty acid-binding protein null and transgenic mice. Am J Physiol Endocrinol Metab 2006;290:E814–23.

25. Hotamisligil GS, Johnson RS, Distel RJ, Ellis R, Papaioannou VE, Spiegelman BM. Uncoupling of obesity from insulin resistance through a targeted mutation in aP2, the adipocyte fatty acid binding protein. Science 1996; 274:1377–9.
26. Zeisberger SM, Odermatt B, Marty C, Zehnder-Fjallman AH, Ballmer-Hofer K, Schwendener RA. Clodronate-liposome-mediated depletion of tumour-associated macrophages: a new and highly effective antiangiogenic therapy approach. Br J Cancer 2006;95:272–81.
27. Van RN, Sanders A. Liposome mediated depletion of macrophages: mechanism of action, preparation of liposomes and applications. J Immunol Methods 1994;174:83–93.
28. Chou J, Shahi P, Werb Z. microRNA-mediated regulation of the tumor microenvironment. Cell Cycle 2013;12:3262–71.
29. Graff JW, Dickson AM, Clay G, McCaffrey AP, Wilson ME. Identifying functional microRNAs in macrophages with polarized phenotypes. J Biol Chem 2012;287:21816–25.
30. Liu S, Wu LC, Pang J, Santhanam R, Schwind S, Wu YZ, et al. Sp1/NFkappaB/HDAC/miR-29b regulatory network in KIT-driven myeloid leukemia. Cancer Cell 2010;17:333–47.
31. Makowski L, Brittingham KC, Reynolds JM, Suttles J, Hotamisligil GS. The fatty acid-binding protein, aP2, coordinates macrophage cholesterol trafficking and inflammatory activity. Macrophage expression of aP2 impacts peroxisome proliferator-activated receptor gamma and IkappaB kinase activities. J Biol Chem 2005;280:12888–95.
32. Chang Q, Bournazou E, Sansone P, Berishaj M, Gao SP, Daly L, et al. The IL-6/JAK/Stat3 feed-forward loop drives tumorigenesis and metastasis. Neoplasia 2013;15:848–62.
33. Sansone P, Bromberg J. Environment, inflammation, and cancer. Curr Opin Genet Dev 2011;21:80–5.
34. Mills CD, Lenz LL, Harris RA. A breakthrough: macrophage-directed cancer immunotherapy. Cancer Res 2016;76:513–6.
35. Murray PJ, Allen JE, Biswas SK, Fisher EA, Gilroy DW, Goerdt S, et al. Macrophage activation and polarization: nomenclature and experimental guidelines. Immunity 2014;41:14–20.
36. Solinas G, Germano G, Mantovani A, Allavena P. Tumor-associated macrophages (TAM) as major players of the cancer-related inflammation. J Leukoc Biol 2009;86:1065–73.
37. Obeid E, Nanda R, Fu YX, Olopade OI. The role of tumor-associated macrophages in breast cancer progression (review). Int J Oncol 2013;43: 5–12.
38. Noy R, Pollard JW. Tumor-associated macrophages: from mechanisms to therapy. Immunity 2014;41:49–61.
39. Shand FH, Ueha S, Otsuji M, Koid SS, Shichino S, Tsukui T, et al. Tracking of intertissue migration reveals the origins of tumor-infiltrating monocytes. Proc Natl Acad Sci U S A 2014;111:7771–6.
40. Arnold L, Henry A, Poron F, Baba-Amer Y, van RN, Plonquet A, et al. Inflammatory monocytes recruited after skeletal muscle injury switch into antiinflammatory macrophages to support myogenesis. J Exp Med 2007;204:1057–69.
41. Nahrendorf M, Swirski FK, Aikawa E, Stangenberg L, Wurdinger T, Figueiredo JL, et al. The healing myocardium sequentially mobilizes two monocyte subsets with divergent and complementary functions. J Exp Med 2007;204:3037–47.
42. Landsman L, Varol C, Jung S. Distinct differentiation potential of blood monocyte subsets in the lung. J Immunol 2007;178:2000–7.
43. Nieman KM, Kenny HA, Penicka CV, Ladanyi A, Buell-Gutbrod R, Zillhardt MR, et al. Adipocytes promote ovarian cancer metastasis and provide energy for rapid tumor growth. Nat Med 2011;17:1498–503.
44. Lee D, Wada K, Taniguchi Y, Al-Shareef H, Masuda T, Usami Y, et al. Expression of fatty acid binding protein 4 is involved in the cell growth of oral squamous cell carcinoma. Oncol Rep 2014;31:1116–20.
45. Qin L, Li R, Zhang J, Li A, Luo R. Special suppressive role of miR-29b in HER2-positive breast cancer cells by targeting Stat3. Am J Transl Res 2015;7:878–90.
46. Yan B, Guo Q, Fu FJ, Wang Z, Yin Z, Wei YB, et al. The role of miR-29b in cancer: regulation, function, and signaling. Onco Targets Ther 2015; 8:539–48.
47. Wu Y, Crawford M, Mao Y, Lee RJ, Davis IC, Elton TS, et al. Therapeutic delivery of MicroRNA-29b by cationic lipoplexes for lung cancer. Mol Ther Nucleic Acids 2013;2:e84.
48. Panni RZ, Linehan DC, DeNardo DG. Targeting tumor-infiltrating macrophages to combat cancer. Immunotherapy 2013;5:1075–87.
49. Williams CB, Yeh ES, Soloff AC. Tumor-associated macrophages: unwitting accomplices in breast cancer malignancy. NPJ Breast Cancer 2016;2.